Assessing the effect of D-xylose on the sugar signaling pathways of *Saccharomyces cerevisiae* in strains engineered for xylose transport and assimilation

Karen O Osiro, Daniel P Brink, Celina Borgström, Lisa Wasserstrom, Magnus Carlquist, Marie F Gorwa-Grauslund*

Applied Microbiology, Department of Chemistry, Lund University, Lund, Sweden

*Corresponding author

E- mail: Marie-Francoise.Gorwa@tmb.lth.se

Abstract

One of the challenges of establishing an industrially competitive process to ferment lignocellulose to value-added products using *Saccharomyces cerevisiae* is to get efficient mixed sugar fermentations. Despite successful metabolic engineering strategies, the xylose assimilation rates of recombinant *S. cerevisiae* remain significantly lower than for the preferred carbon source, glucose. Previously we established a panel of *in vivo* biosensor strains (TMB371X) where different promoters (*HXT1/2/4p; SUC2p, CAT8p; TPS1p/2p, TEF4p*) from the main sugar signaling pathways were coupled with the yEGFP3 gene, and observed that wild type *S. cerevisiae* cannot sense extracellular xylose. Here we expand upon these strains by adding a mutated galactose transporter (*GAL2-N376F*) with improved xylose affinity (TMB372X), and both the transporter and an oxido-reductase xylose pathway (TMB375X). On xylose, the TMB372X strains displayed population heterogeneities, which disappeared when carbon starvation was relieved by the addition of the xylose assimilation pathway (TMB375X). Furthermore, the signal in the TMB375X strains on high xylose (50 g/L) was very similar to the signal recorded on low glucose (≤ 5 g/L). This suggests that

intracellular xylose triggers a similar signal to carbon limitation in cells that are actively metabolizing xylose, in turn causing the low assimilation rates.

Keywords

Saccharomyces cerevisiae; sugar sensing/signaling; xylose; XR/XDH; GFP biosensor; cAMP/PKA; Snf3p/Rgt2p; SNF1/Mig1p; flow cytometry

One-sentence summary

In this study, *in vivo* single-cell biosensors were used to assess the sensing of glucose and xylose sugars by *Saccharomyces cerevisiae*, in order to understand its low xylose utilization rate.

Background

The lignocellulose-based biorefinery has been foreseen as a candidate process to supply the future global demand for sustainable energy sources that can replace the non-renewable sources used today, and has shown good potential to decrease the environmental impact compared to the conventional processes (Uihlein and Schebek 2009). Up to one third of the composition of lignocellulose is constituted of D-xylose, the second most abundant sugar in Nature (Limayem and Ricke 2012), meaning that in order to fully take advantage of the carbon content of this renewable feedstock, future biorefineries will require microbes that can efficiently convert not only hexose (C_6), but also pentose (C_5) sugars such as xylose, preferably simultaneously. Although some microorganisms are naturally able to ferment and produce valuable chemical compounds from xylose, they are seldom suitable for industrial applications due to their poor performance under high osmotic stress, low pH, strict anaerobic environments and/or in the presence of the wide range of inhibitory compounds released during lignocellulose pretreatment (Hahn-Hägerdal, et al. 2007a, Kwak and Jin 2017, Rudolf, et al. 2008, Skoog and Hahn-Hägerdal 1988). Instead, the industrially robust, natural ethanol producing organism *Saccharomyces cerevisiae* (Baker´s yeast) has for a long time been

considered a promising host for metabolic engineering to enable pentose conversion (Jeffries and Jin 2004, van Maris, et al. 2007).

Over the years, different strategies have been developed in order to introduce and improve xylose metabolism in *S. cerevisiae*. As the endogenous genes for xylose catabolism already present in this yeast are insufficiently expressed (Attfield and Bell 2006, Toivari, et al. 2004), exogenous genes from natural xylose assimilating microbes have been used to enable pentose catabolism in *S. cerevisiae* (Brat, et al. 2009, Kötter, et al. 1990, Kötter and Ciriacy 1993). The oxido-reductase pathway that was used in the present study consists of a xylose reductase (XR) and a xylitol dehydrogenase (XDH) that converts xylose to xylulose via xylitol; xylulose can then enter the non-oxidative pentose phosphate pathway (PPP) via the endogenous xylulokinase (XK) and be further shunted to the central carbon metabolism (Kötter and Ciriacy 1993). Xylose utilization can be further improved by also overexpressing the endogenous *TAL1* and *TKL1* genes in order to increase the metabolic flux through the PPP (Hahn-Hägerdal, et al. 2007b).

Despite these modifications, growth and productivity is still significantly lower on xylose than on glucose (Hahn-Hägerdal, et al. 2007a). Redox imbalance is an issue with the oxido-reductase pathway, as the commonly used *Scheffersomyces stipitis* XR has a higher preference for NADPH over NADH while the XDH is strictly NAD^+-dependent, resulting in an insufficient recycling of NADPH and NAD^+ (Bruinenberg, et al. 1983, Kötter and Ciriacy 1993). However, the recently identified XR of *Spathaspora passalidarum* (encoded by *XYL1.2*) which prefers NADH over NADPH can be used to significantly decrease the redox issues of the XR/XDH pathway in *S. cerevisiae* (Cadete, et al. 2016).

Co-fermentation of hexose and pentose sugar also prove challenging as glucose is preferentially consumed over xylose (Moysés, et al. 2016, Zaldivar, et al. 2002), because of the lack of specific xylose transporters (Kim, et al. 2012). Although xylose can be taken up by some of the native hexose transporters, during mixed sugar cultivations, these transporters have a naturally higher affinity for glucose (Hamacher, et al. 2002, Kotyk 1967). Nevertheless, a couple of recent studies have demonstrated improved xylose uptake by engineering hexose and galactose transporters for improved xylose specificity (Apel, et al. 2016, Farwick, et al. 2014, Nijland, et al. 2014, Nijland, et al. 2016).

At the present stage, xylose can be fermented to ethanol by recombinant *S. cerevisiae*, but at such low rates that it has been hypothesized that xylose still is not recognized as a fermentable sugar (Bergdahl, et al. 2012, Feng and Zhao 2013, Jin, et al. 2004, Klimacek, et al. 2010, Runquist, et al. 2009, Salusjarvi, et al. 2006). This indicates possible issues with the intra- and/or extracellular sensing of xylose in *S. cerevisiae*. A handful of studies have shown the influence of xylose on glucose signaling (Alff-Tuomala, et al. 2016, Fernandez, et al. 1986, Jin, et al. 2004, Salusjarvi, et al. 2006, Salusjärvi, et al. 2008, Zeng, et al. 2016), but the mechanism by which *S. cerevisiae* could potentially sense xylose is still mainly unknown. Therefore, increased comprehension of the xylose effect on the main glucose signaling pathways may lead to new strategies for enhancing xylose utilization.

There are three main signaling pathways that control glucose sensing in *S. cerevisiae* (Figure 1): the Snf3p/Rgt2p pathway, the SNF1/Mig1p pathway and the cAMP/PKA pathway (Santangelo 2006). We recently reported on the construction of a panel of fluorescent biosensors strains that allows for real-time single-cell monitoring of these three signaling pathways during different carbon conditions. The promotor regions of eight different genes (*HXT1/2/4p; SUC2p, CAT8p; TPS1/2p, TEF4p*) - each controlled by one of the three signaling pathways - were coupled to the *yEGFP3* (yeast Enhanced Green Fluorescent Protein) reporter gene and integrated in the chromosome in single-copy (Brink, et al. 2016). The *HXT1/2/4p* biosensors represent the Snf3p/Rgt2p pathway, which regulates the expression of hexose transporters by sensing extracellular glucose (Boles and Hollenberg 1997, Santangelo 2006, Özcan, et al. 1998). The *SUC2p* and *CAT8p* biosensors are reporters for the SNF1/Mig1p pathway that is responsible for carbon catabolite repression and is regulated mainly by intracellular glucose. This pathway can induce genes for alternative carbon source utilization during glucose depletion (Santangelo 2006, Özcan, et al. 1997). The *TPS1/2* promoters represent the cAMP/PKA pathway, which responds to both internal and external glucose and governs, among others, the gluconeogenesis and environmental stress response (Rolland, et al. 2002, Santangelo 2006). The Protein Kinase A (PKA) is activated in the presence of glucose, which leads to a phosphorylation of several metabolic enzymes, transcription factors, and, consequently, gene regulation (Kim, et al. 2003, Kraakman, et al. 1999, Mosley, et al. 2003, Santangelo 2006). It has also been demonstrated that *SUC2* and *HXT1* are in part regulated by the cAMP/PKA pathway, meaning that these signaling

pathways are cross-talking (Gancedo, et al. 2015, Kaniak, et al. 2004, Kim and Johnston 2006).

Previously, we applied the biosensor strains to investigate whether the signal on glucose differentiated from that on xylose in any of the three signaling routes in non-xylose metabolizing *S. cerevisiae*. It was found that the biosensors remained unresponsive to extracellular xylose, and that certain population heterogeneities indicated that xylose that had been internalized (e.g. through promiscuous hexose transporters) was being sensed by some parts of the glucose signaling pathway (Brink, et al. 2016). The current study pursues the investigation of the sugar signaling response of *S. cerevisiae*, this time for strains where a transporter with increased affinity for xylose is overexpressed (Farwick, et al. 2014), or for strains that can fully metabolize xylose, by addition of the same transporter gene, the XR/XDH xylose pathway gene and overexpressed *TAL1* and *TKL1* genes in the PPP (Figure 2).

Materials and Methods

Strains

The yeast strains used in the study are based on previously constructed biosensors strains (Brink, et al. 2016), and are described in Table 1. Strains TMB3701-TMB3709 are collectively referred as TMB370X strains and this nomenclature is also used for the different series of derived strains (e.g. TMB371X, TMB372X and TMB375X; Table 1). Depending on the experimental requirements, the strains were grown on either Yeast Peptone Dextrose (YPD; yeast extract 10 g/L, peptone 20 g/L, glucose 20 g/L) or Yeast Nitrogen Base (YNB; 6.7 g/L Yeast Nitrogen Base without amino acids; Becton–Dickinson, NJ, US) supplemented with different carbon sources (detailed below). *Escherichia coli* NEB5-α (New England BioLabs, Ipswich, MA, US) was used for routine plasmid sub-cloning and was cultivated in Lysogeny Broth (LB) medium (10 g/L tryptone, 5 g/L yeast extract, 5 g/L NaCl, pH 7.0). Solid plates were obtained by adding 15 g/L agar-agar to the above media. All strains were stored at -80°C in 25 % (v/v) glycerol; CRISPR-Cas9 transformants were stored in the presence of their respective antibiotics (detailed below).

Molecular biology methods

All cloning procedures were performed according to standard molecular biology methods (Sambrook and Russell 2001). Genomic yeast DNA was extracted according to the LiOAc-SDS method (Lõoke, et al. 2011) and PCR products were purified with GeneJET PCR purification kit (Thermo Scientifc, Waltham, MA, US). All primers (S1 Supporting Information Table S5) were obtained from Eurofins MWG Operon (Ebersberg, Germany). Restriction enzymes, T4 ligase and Phusion DNA polymerase were purchased from Thermo Scientific (Waltham, MA, US), except for *Zra*I that was purchased from New England Biolabs (Ipswich, MA, US). Plasmid purification was performed with GeneJET plasmid MiniPrep kit (Thermo Scientific, Waltham, MA, US).

The lithium acetate transformation protocol (Gietz and Schiestl 2007), modified with the addition of DMSO (10% v/v) prior to heat shock (Hill, et al. 1991), was used for all the *S. cerevisiae* transformations. Competent *E. coli* cells were prepared and transformed according to the method of Inoue and colleagues (Inoue, et al. 1990). Selection of *E. coli* transformants was performed on LB medium supplemented with 50 µg/mL of ampicillin.

Plasmids and transformation fragments

The plasmids that were used in the study are listed in Table 2. The *TDH3p-GAL2_N376F-CYC1t* cassette containing the mutated *GAL2* transporter (*GAL2-N376F*) was constructed from the pRS62N_*GAL2_N376F* plasmid (Farwick, et al. 2014) that was a gift from Prof. E. Boles. Since the antibiotic marker and truncated *HXT7p* promoter in pRS62N_*GAL2_N376F* was not desired in the current study, the *GAL2_N376F* cassette was cloned into a new vector. This was made in two steps: first, the cassette was amplified from the original plasmid using the GAL2-F1_SmaI and GAL2_R1_XhoI primers and was ligated between the *TDH3* promoter and the *CYC1* terminator in the p426-GPD Mumberg vector (Mumberg, et al. 1995), thus generating the p426-*GPD-GAL2_N376F* plasmid; second, the *TDH3p-GAL2_N376F-CYC1t* cassette was amplified from p426-*GPD-GAL2_N376F* plasmid using the TDH3p-F2-SacI and CYC1t-R2-SphI primers. The final plasmid (YIplac128-*GAL2_N376F*) was constructed by ligating the *TDH3p-GAL2_ N376F-CYC1t* cassette to YIplac128 (*LEU2*) using the *Sac*I and *Sph*I restriction sites.

Construction of the *XR-XDH-XK* integrative plasmids

S. cerevisiae promotors *TEF1p* and *PGI1p,* terminators *GPM1t* and *PYK1t,* as well as the *XKS1* ORF encoding xylulokinase (Ho, et al. 1998), were PCR amplified individually from genomic DNA isolated from *S. cerevisiae* CEN.PK 113-7D with primers generating a 40 bp homology between promoter, gene and terminator. *Scheffersomyces stipitis* gene *SsXDH* encoding xylitol dehydrogenase (Kötter, et al. 1990) was amplified from the plasmid YIpRC5 (Cadete, et al. 2016). Following agarose gel electrophoresis, the amplified PCR products were gel-purified. Each individual gene expression cassette (*TEF1p-SsXDH-GPM1t* and *PGI1p-XKS1-PYK1t*) was assembled by overlap extension PCR (OE-PCR) using primer pairs 65/70 (*XDH* cassette) and LW71/76 (*XKS1* cassette) with each part added in equimolar amounts. In order to enable In-fusion HD cloning (In-Fusion® HD Cloning Kit User Manual, Clontech Laboratories, California, USA), 15 bp homology regions between the two cassettes and the plasmid YIpRC5 was included in the primers. Following electrophoresis, the OE-PCR products were gel-purified. 2 µg of plasmid YIpRC5, already carrying the *SpXYL1.2* gene cassette for XR from *Spathaspora passalidarum,* was cleaved with Fastdigest *Pst*I and *Sac*I and separated by gel electrophoresis followed by gel-purification (GeneJet Gel Extraction Kit; Thermo Scientifc, Waltham, MA, US). Gene cassettes and *Pst*I/*Sac*I digested YIpRC5 containing the remaining XR encoding gene were added in equimolar amount to 5×In-fusion HD enzyme premix following the In-fusion HD cloning kit user manual (Raman and Martin 2014). The obtained plasmid was verified using restriction enzymes *Sac*I and *Pst*I and agarose gel electrophoresis. The plasmid was Sanger sequenced (Eurofins MWG Operon; Ebersberg, Germany) using primers 78-83 and named pLWA20.

The xylose pathway from pLWA20 was recloned into pCfB2899, pCf3037 and pCf3040 to allow integration of three copies of the cassette using a CRISPR-Cas9 system into the intergenic regions X-2, XI-5 and XII-4, respectively (Jessop-Fabre, et al. 2016), resulting in plasmids pLWA31, pLWA32 and pLWA33. To construct pLWA32 and pLWA33, the XR/XDH/XKS1 ORFs were amplified from pLWA20 using primers 247/248 that contained sites for *Asc*I and *Sbf*I while the pCfB2899/pCfB3040 backbone was amplified using primers 239 and 240 followed by cleaving with *Asc*I and *Sbf*I. The template vector was removed by *Dpn*I cleaving. All fragments were gel-purified after cleaving and subsequently ligated. The resulting plasmids were verified by PCR using primers 245/246 for pLWA32 (pCfB2899-pLWA20) and 244/246 for pLWA33 (pCfB3040-pLWA20) and by restriction digest with

Fastdigest *Smi*I. The resulting plasmids were sequenced using primers LW79-83. To clone the xylose pathway cassette into pCfB3037 XDH, XKS1 and XR was cleaved out from pLWA20 using *Asc*I/*Pmi*I and the 6642 bp fragment was purified from the gel. The plasmid backbone of pCfB3037 (including the 5' and 3' genomic target sequences XI-5) was amplified using primers 239 and 240 and cleaved with *Msc*I/*Asc*I. The template vector was removed by *Dpn*I cleaving. All fragments were gel-purified after cleaving and subsequently ligated. The obtained plasmid, pLWA31, was verified by restriction digest using *Smi*I and by sequencing using primers that anneal in the plasmid backbone and the *TDH3*p region (Seq_forward, Seq_reverse and TDH3p-F2-SacI).

Construction of the *TKL-TAL* integrative plasmid (pLWA19)

S. cerevisiae promotors *FBA1p* and *TPI1p*, terminators *PDC1t* and *CPS1t* and the *TKL1* and *TAL1* ORFs were PCR amplified individually from *S. cerevisiae* CEN.PK 113-7D genomic DNA generating 40 bp homology between promoter, gene and terminator. Following agarose gel electrophoresis, the amplified PCR products were gel-purified (Thermo Scientifc, Waltham, MA, US). Each individual gene expression cassette (*FBA1p-TKL1-PDC1t* and *TPI1p-TAL1-CPS1t*) was assembled by OE-PCR using primer pairs 45/50 (*TKL1*) and 51/56 (*TAL1*) with each part added in equimolar amounts. To enable In-fusion HD cloning, as described above for pLWA20, 15 bp homology regions between the two cassettes and the plasmid pUG-amdSYM (Solis-Escalante, et al. 2013) was included in the primers. Following agarose gel electrophoresis, the OE-PCR products were gel-purified. 2 µg of plasmid pUG-amdSYM2 was cleaved with *Spe*I and *Sac*II and gel-purified. Gene cassettes and *Spe*I/*Sac*II digested pUG-amdSYM2 were added in equimolar amount to 5×In-fusion HD enzyme premix following the In-fusion HD cloning kit user manual (Raman and Martin 2014). The plasmid was verified by sequencing using primers 5, 51, 57-60 and was named pLWA19.

pLWA19 was designed to be cleaved with *SfaA*I and *Not*I and integrated by nested double homologous integration aided by 5' and 3' homologous targeting fragments. Fragments for integration of the resulting *TKL-TAL(SfaA*I/*Not*I*)* cassette in the *VAC17/MRC1* intergenic locus were amplified from W303 genomic DNA using the following primers: 88_f and 107_r for the 5' *VAC17/MRC1* fragment and 108_f and MRC1_TF_r for the 3' *VAC17/MRC1* fragment.

Strain generation

TMB72X series

The TMB372X strains containing the different biosensors together with the mutated Gal2p transporter were constructed from the TMB370X (*Leu*$^-$) strains by integration of the YIplac128-GAL2_N376F (*Leu*$^+$) plasmid at the *SPB1/PBN1* intergenic locus. This locus was previously used to cure the leucine auxotrophy with an empty YIplac128 plasmid (*LEU2)* in the TMB371X strains (Brink, et al. 2016), meaning that all yeast strains in this study have a comparable genetic makeup in this region. Targeting fragments for double homologous integration of the YIplac128-*GAL2_N376F* plasmid (linearized with *Zra*I) were PCR amplified using the SPB1_ Targ1_F/SPB1_ Targ1_Rtail and PBN1_ Targ2_Ftail/PBN1_ Targ2_R primer pairs, and were used for single-copy integration into the yeast genome as previously described (Brink, et al. 2016).

TMB375X series

The TMB372X strains were used to construct the TMB375X strains by sequential integration of a cassette for overexpression of *TKL1* and *TAL1* genes, followed by three copies of the cassette containing the xylose pathway genes (*SpXYL1.2, SsXDH* and *XKS1*). These integrations were performed using a *S. cerevisiae* CRISPR-Cas9 system (Stovicek, et al. 2015). First, the different TMB372X strains were transformed with the pCfB2312 plasmid containing the Cas9 gene (Stovicek, et al. 2015) and selected for on YPD with 200 µg/mL geneticin. Following this, the *TKL-TAL(SfaA*I/*Not*I*)* fragment was inserted in the *VAC17/MRC1* intergenic region. 1µg gRNA plasmid (pLWA26), 2µg linear DNA fragments of *TKL-TAL(SfaAI*/*NotI)* and 0.5 µg of each 5'/3' targeting fragments were used and strains were selected for with 200 µg/mL geneticin and 100 µg/mL clonNAT. Cultivations in YPD with 200 µg/mL geneticin only (i.e. without clonNAT) were performed to cure the cells of the pLWA26 gRNA plasmid prior to the next transformation. Second, the xylose pathway genes were integrated in three different intergenic loci: X-2 (chrX; *NCA3/NSF1*), XI-5 (chrXI; *FRE2/COS9*) and XII-4 (chrXII; *NIT3/YLR352W*) (Jessop-Fabre, et al. 2016). 1µg gRNA plasmid (pCfB3053; Jessop-Fabre, et al. (2016)), and 1µg of each *Smi*I linearized plasmid (pLWA31, pLWA32 and pLWA33) were used and transformants were selected on YPD with 200 µg/mL geneticin and 100 µg/mL clonNAT. Correct integration of pLWA31 (XI-5),

pLWA32 (X-2) and pLWA33 (XII-4) was verified using primer pairs 246/250, 246/249 and 246/251, respectively.

Sampling and analysis

Enzymatic assays

Single yeast colonies from the TMB375X strains (maintained on YPD agar plates with 200 µg/mL geneticin) were used to inoculate 5 mL of YPD medium in 50 mL conical centrifuge tubes. Cells were grown overnight at 30°C and 180 rpm and were harvested at 3000 rpm for 5 minutes. The whole-cell protein was extracted by treating the cell pellet with Y-PER (Yeast Protein Extraction Reagent; Pierce, Rockford, IL, USA) according to the manufacturer's instructions. The Micro-BCA kit (Pierce, Rockford, IL, USA) and Bovine Albumin standard (Thermo Fisher Scientific, Waltham, MA, USA) were used to determine the total protein concentration.

Xylose reductase (XR) and xylitol dehydrogenase (XDH) microtiter plate assays were adapted from previous protocols (Rizzi, et al. 1989, Smiley and Bolen 1982). XR activity was determined by following NADH oxidation at 340 nm on a Multiskan Ascent (Thermo Electro Corporation, Finland) with constant read-mode (one measurement every 3 seconds, 60 measurements points in total). The reaction consisted of 100 mM triethanolamine pH 7.0, 0.2 mM NADH, 350 mM xylose as a substrate and 5 µL sample (protein extract from the TMB375X strains) for a total reaction volume of 250 µL, and was initiated by the addition of the substrate. XDH activity was assayed with the same setup, but NAD^+ reduction was now followed. The assay (250 µL total volume) consisted of 100 mM glycine pH 9.0, 50 mM $MgCl_2$, 0.3 mM NAD^+, 150 mM xylitol as a substrate and 5 µL sample. The specific activity was defined as the amount of enzyme required to catalyze the formation/disappearance of 1µmol of NADH (εNADH = 6220 L/mol.cm) per min and mg protein (Burnett 1972, Horecker and Kornberg 1948). The enzymatic assays were done in biological duplicates and technical triplicates.

Growth curve

Single colonies from the TMB375X strains were inoculated in 5 mL of YPD medium in a 50 mL tubes for overnight cultivation at 30°C, 180 rpm. The cells were then inoculated in a pre-sterilized Microtest Plate 96 Well R (Sarstedt, Nümbrecht, Germany) with YNB medium supplemented with either 20 g/L glucose or 20 g/L xylose. A starting Optical Density at 620nm (OD_{620}) of 0.5 and a total volume of 240 µL were used. The plate was shaken at 1000 rpm in a 30°C incubator. Measurements were taken every hour for 8 hours in total. YNB medium without cells and supplemented with the carbon source used for each specific growth curve was used as a negative control. Growth was recorded in biological duplicates and technical triplicates.

Flow cytometry analysis

A BD Accuri C6 flow cytometer equipped with a BD CSampler autosampler (Becton–Dickinson, NJ, US) was used to analyze the single-cell fluorescence intensity (FI) of the TMB372X and TMB375X GFP-reporter strains on different carbon sources. Cells were inoculated in YNB medium buffered with 50 mM potassium hydrogen phtalate at pH 5.5 (from here on denoted as YNB-KHPthalate medium) complemented with one of the following: xylose 50 g/L, xylose 5 g/L, xylose 50 g/L with glucose 5 g/L, glucose 5 g/L. A 488 nm excitation wavelength and 533/30 bandpass filter (from here on referred as the *FL1-H channel*) were used. The setup and handling of the Accuri flow cytometer was performed as previously reported (Brink, et al. 2016). Data analysis was performed with the FlowJo software (v10; Treestar, Inc., San Carlos, CA). Although TMB37X1 did not contain any biosensor, repression and induction were performed in glucose 40 g/L and glucose 1 g/L, respectively, in order to assess the auto-fluorescence under different conditions.

Two pre-cultivations were performed prior to the flow cytometry assay in order to gain sufficient biomass and biosensor repression at time 0h of the experiment. The repression was performed to establish a FI baseline with an as low as possible intensity at the start of the experiment. Pre-pre-cultivations were prepared by inoculating a single colony in 5 mL of YNB-KHPhtalate complemented with glucose 20 g/L (50 mL conical tubes) and incubation

for 14 h at 30°C and 180 rpm. Following this, the strains were submitted to a pre-cultivation in repressing conditions according to the known regulatory conditions of each biosensor promoter (Table 3). Cells were inoculated in 5 mL (in 50 mL conical tubes) at and initial OD_{620} of 0.05 and were grown for 14 h. The strains were analyzed with the previously developed microtiter plate protocol (Brink, et al. 2016), with some improvements regarding the repression and induction conditions for some of the biosensor strains (Table 3). The *TEF4p* biosensor proved challenging to repress, and the cells were therefore cultivated from an initial OD_{620} of 0.1 for 26h on YNB-KHPthalate supplemented with ethanol 3% (v/v) as a repressing condition; for the inducing condition, YNB-KHPhtalate with glucose 20 g/L was used. For the repressing condition of the *HXT1p* biosensor, cultivations for 14h in YNB-KHPhtalate with glucose 5g/L were used. For each strain and condition, biological triplicates and technical duplicates were performed.

Population heterogeneities on the GFP channel (FL1-H) were identified numerically and classified into low and high FI populations using two-component Gaussian Mixture modeling. The analysis was performed with Matlab (Release R2015a, The MathWorks, Inc., Natick, MA, US) and is further outlined in S1 Supporting Information.

Results

Strain construction and validation

We previously reported on the construction and validation of a non-invasive fluorescent *in vivo* reporter system for real-time monitoring of the three major glucose signaling pathways in *S. cerevisiae* (Brink, et al. 2016). The present study complements the previous work by expanding the biosensor panel with sixteen new strains divided in two strain series: TMB372X and TMB375X (Table 1). The TMB372X strains contains the different GFP-coupled biosensors from the previous study (*HXT1/2/4p, SUC2p, TPS1p/2p, TEF4p*) together with a mutated galactose transporter (*GAL2*-N376F). This transporter has been reported to have increased affinity for D-xylose while having lost the ability to transport hexoses (Farwick, et al. 2014). The TMB372X strains were constructed from the TMB370X (*Leu*$^-$) series by integration of the *GAL2* mutated gene at the *SPB1/PBN1* intergenic locus with *LEU2* as the selection marker. The TMB375X strains were then constructed from the TMB372X

strains by overexpressing two of the non-oxidative pentose phosphate pathway genes (*TAL1* and *TKL1*) and integrating three gene copies of an oxido-reductase xylose pathway (*XR-XDH-XK*; cf. Table 1 & the *Material and Methods* for details). All integrations were verified using yeast colony PCR.

In order to ascertain the in-series comparability of the strains of the TMB375X series, the XR and XDH enzymatic activities were assayed, and it was confirmed that the activities of the respective enzymes were all in the same range across all strains (S1 Supporting Information, Figure S3). Likewise, growth experiments in glucose 20 g/L or xylose 20 g/L were also performed, and all strains demonstrated a similar growth pattern and -rate (S1 Supporting Information, Table S6 and Figure S2).

Screening of the biosensor response to glucose and xylose

The strains from this and the previous studies were designed to analyze the effect of xylose on biosensors for three different scenarios for the uptake and metabolism of xylose (Figure 2): extracellular xylose only, intracellular non-metabolized xylose and intracellular metabolized xylose. The wild type, non-xylose utilizing TMB371X strains (Figure 2A) were used to assess the effect of xylose on the sugar signaling when most of xylose was extracellular (Brink, et al. 2016). The previous study on these strains indicated that *S. cerevisiae* did not sense extracellular xylose, but that there was a response towards intracellular xylose, possibly transported inside the cell by hexose transporters capable to also transport xylose to some degree (Brink, et al. 2016). In the current study, the TMB372X strains were used to analyze the biosensor response when xylose could efficiently be transported inside the cell via an engineered transporter, although it was not further metabolized (Figure 2B). The final case (intracellular metabolized xylose) was assessed with the TMB375X strains, containing the transporter as well as a recombinant pathway for xylose assimilation (Figure 2C).

The induction and repression conditions used in this study were performed as previously described (Brink, et al. 2016) with slight modifications to improve the repression profile of the *HXT*1p and *TEF4*p biosensor strains (Table 3). The results of the flow cytometry screening of the biosensor strains on different concentrations of glucose and xylose are presented in Figure 3 (TMB372X strains) & Figure 4 (TMB375X strains). The corresponding data analysis - including peak means, coefficient of variation (CV) and subpopulation identification - for all strains and replicates is found in S1 Supporting Information Table S1-4.

The fold change results of the TMB375X (transporter + assimilation) strains are also summarized in heat map form in Figure 5 (see also S1 Supporting Information Figure S4 for an extended heat map with all strains of TMB371X-5X). It was found that the assessed biosensors were repressed and induced on glucose as expected (Table 3; Figure 3 & 4). However, not all strains could be completely repressed (dotted vertical red line in Figure 3 & 4), meaning that they had higher fluorescence than the cellular auto-fluorescence intensity of the control strains without GFP (black vertical line in Figure 3 & 4). This was previously observed for the strains TMB371X (Brink, et al. 2016), and was therefore not an attribute of the added genetic constructs in strains TMB372X (transporter) and TMB375X (transporter + assimilation). This discrepancy between repression and auto-fluorescence signal was mainly observed for the *HXT*2p, *TPS1/2*p and *TEF4*p biosensors (Figure 3 & 4: C, F, G and H).

A shift in intensity and/or population heterogeneity was observed for the TMB3721 strain, the negative control strain without GFP that was used to determine the cellular auto-fluorescence. When inoculated in low glucose concentration (1 and 5 g/L) and/or in xylose (that the strain cannot metabolize), a decreased fluorescence was emitted compared to the control conditions for induction and repression (Figure 3A, histograms I and R). TMB3751, the negative control that was able to grow on xylose, instead displayed a fluorescence intensity (FI) for xylose conditions comparable the repressing condition (Figure 4A). The variations in auto-fluorescence observed for the TMB3721 strain can likely be explained by a decrease/variation in cell size due to carbon limitation due to low glucose concentration and the lack of xylose metabolism.

The biosensors for the Snf3p/Rgt2p signaling pathway gave a partial response in the presence of xylose. Both strains with the sensor for the *HXT1*p low-affinity hexose transporter (TMB3722 and TMB3752) showed a slightly higher fluorescence for the mixture of xylose 50 g/L and glucose 5 g/L, but no change in signal was detected for glucose 5 g/L, xylose 5 g/L or xylose 50 g/L (Figure 3B & 4B). *HXT2*p and *HXT4*p, the high-affinity hexose transporters, behaved similar to each other but with population heterogeneities detected in the presence of xylose, for the xylose transporter strains TMB3723 and TMB3724 (Figure 3C & 3D; Supporting Information Table S1). However, when the xylose pathway was added (TMB3753 and TMB3754), a distinctive change in signaling pattern was observed with the disappearance of the subpopulations (Figure 4C & 4D; Supporting Information Table S2); this was also

manifested in the TMB375X heat map (Figure 5), where the two strains showed an induction signal on xylose similar to the inducing control condition (glucose 1 g/L). Cultivating the biosensors on YNB medium without any carbon source did not impact the signal response in any of the strains (Supporting Information Table S7), meaning that the observed response on xylose can be attributed to xylose itself and not to a lack of (recognizable) carbon.

The promoter of the invertase-encoding gene *SUC2* was chosen as a representative biosensor for the SNF1/Mig1p signaling pathway; the previously assayed *Cat8p* as a potential sensor for this pathway (Brink, et al. 2016) was not considered this time since it behaved like *SUC2p* but with lower overall FI, therefore giving less resolution. The *SUC2p* biosensor was slightly affected by the presence of low xylose concentration (5 g/L) when strain TMB3725 (transporter) was analyzed (Figure 3E). In TMB3755 (transporter + assimilation), metabolized xylose clearly induced this biosensor both in a high or low concentration but with different FI intensity (Figure 5), whereas it was less induced by the mixture of xylose 50 g/L and glucose 5 g/L, and by glucose 5 g/L (Figure 4E, Figure 5).

The biosensors for the cAMP/PKA signaling pathway were not induced by intracellular non-metabolized xylose (TMB3727-28). In fact, the left subpopulation of the *TPS1/2*p strains was more repressed during xylose conditions than during the repression condition (Figure 3F & 3G; S1 Supporting Information Table S1). Nevertheless, when the strains carrying the *TPS1/2*p biosensors were engineered to metabolize xylose (TMB3757-58), the population heterogeneities disappeared, and xylose triggered a small induction (Figure 4F & 4G; S1 Supporting Information Table S). In the case of *TEF4*p, only the strain that was able to metabolize xylose (TMB3759) was induced by high xylose (xylose 50 g/L) (Figure 4I). As was also reported in the previous study (Brink, et al. 2016), the *TEF4*p biosensor is very challenging to repress, which is evident when compared with other biosensors, and especially with the control TMB3751 lacking GFP (Figure 4).

The main difference observed between the two strain series, TMB372X (transporter) and TMB375X (transporter + assimilation), was that the subpopulations that appeared in the TMB372X strains in some of the conditions, often disappeared after the xylose assimilation capacity was added (TMB375X strains; S1 Supporting Information Table S2). Most of the TMB375X biosensors were induced by sole xylose, except for *HXT1p* which did not demonstrate any influence from xylose 5 g/L or 50 g/L; in fact, no major change could be

seen between the histograms of TMB3722 and TMB3752. For the strains that could metabolize xylose (TMB375X) and are known to be induced by glucose 1 g/L (*HXT2p, HXT4p, SUC2p, TPS1p* and *TPS2p*; Table 3), it was noticed that the chosen induction condition resulted in a similar response as with xylose 50 g/L, causing GFP expression for these biosensors under both conditions (Figure 5).

Discussion

Although metabolic engineering has conveyed and improved xylose assimilation in *S. cerevisiae*, xylose utilization rates are still low in comparison to the native glucose assimilation rates (Matsushika, et al. 2009). As a number of studies have suggested that xylose is not recognized as a fermentable sugar by recombinant *S. cerevisiae* strains (Jin, et al. 2004, Salusjarvi, et al. 2006, Salusjärvi, et al. 2008, Zeng, et al. 2016), we created a system of *in vivo* biosensors to investigate how xylose influences the sugar signaling pathways in Baker's yeast (Brink, et al. 2016) and analyze them in conjunction with engineered xylose transport and assimilation. The major outcomes are discussed below.

Population heterogeneity on xylose is alleviated in the transporter strains after the xylose pathway is introduced

The *in vivo* biosensor system was designed with single-copy integration for single-cell measurements, meaning that any population heterogeneity/subpopulation in the GFP data are of physiological relevance, and not artifacts of the biosensor design (Brink, et al. 2016). In the first generation of biosensors (TMB371X; no transporter nor xylose pathway), we have previously observed an effect of internalised xylose on *HXT2/4*p sensors. Subpopulations were only observed for the *HXT2/4p* biosensors during xylose conditions (25 g/l and 50 g/L), and not for any other strains or conditions (Brink, et al. 2016).

In the present study it was found that the addition of the mutated *GAL2* transporter gene (TMB372X) resulted in population heterogeneities in more strains than just the *HXT2/4*p biosensors on xylose 5 g/L and on xylose 50 g/L (Figure 3). It was then observed that these heterogeneities were alleviated after the xylose pathway was added (TMB375X), as the biosensors induced by low glucose (1 g/L) were completely induced in high xylose (50 g/L) when the strains became able to metabolize xylose (Figure 4). The overall disappearance of

the subpopulations in the TMB375X strains able to grow on xylose indicate that it could be either the intracellular xylose and/or the background expression of the yeast's endogenous xylose metabolism (Toivari, et al. 2004) that are behind these heterogeneities.

Xylose resulted in a similar signal to that of limited glucose conditions in strains able to metabolize xylose

Assessment of the xylose sensing in the *S. cerevisiae* strains engineered to transport and grow on xylose (TMB375X) revealed a link between the signal during xylose conditions and the signal at glucose 1 g/L (Figure 4). As the population heterogeneities disappeared in favor of a more homogenous population distribution in TMB375X (S1 Supporting Information Table S2), it became evident that, for sensors induced by low glucose, the signal on both xylose 50 g/L and 5 g/L was highly similar to the signal of low glucose (Figure 4). This is intriguing since it indicates that when *S. cerevisiae* senses intracellular and metabolized xylose, it triggers a low glucose-response that might actually hinder efficient xylose utilization.

*HXT1*p was the only biosensor which did not show population heterogeneity in any of the three constructions (Figure 2): the wild type strains (TMB371X), the Gal2p mutant strains (TMB372X) or the strains in which xylose can be both taken up and metabolized (TMB375X), see Figure 3B and 4B. *HXT1*p is also the only biosensor in this panel that is repressed by low glucose (Table 3), and this effect was also achieved by high xylose (Figure 4B). It is known that the expression of *HXT1* is well-regulated by different proteins of the sugar sensing pathways - Snf3p/Rgt2p (Rgt1p), SNF1/Mig1p (Hxk2p), cAMP/PKA (PKA and Rgt1p) – and the osmotolerance pathway Hog1/MAPK (Sko1p) (Kim and Johnston 2006, Palomino, et al. 2005, Tomás-Cobos, et al. 2004). Therefore, we cannot currently elucidate if the xylose repression on Hxt1p is a result of a) the internalized and metabolized xylose; b) the lack of extracellular glucose signal; or both. Although the *HXT1p* biosensor did not show an induction neither for extracellular, intracellular and metabolized xylose, nor for glucose 5 g/L, the induction effect observed on the mix of glucose 5 g/L and xylose 50 g/L (Figure 3B and 4B) might be caused by the high molarity from xylose 50 g/L along combined with effects of the cell sensing glucose. The Hog1/MAPK pathway is activated during conditions of high osmotic stress (e.g. high concentrations of sugars or salts), and regulates among other targets Sko1p which is a repressor of *HXT1* (Figure 1B). Upon activation of Hog1/MAPK, Sko1p is

phosphorylated and released from the *HXT1* promoter, allowing the expression of the gene (Tomás-Cobos, et al. 2004).

HXT2/4p are known to be repressed during glucose absence (by e.g. Rgt1p), and also at high glucose concentrations (by e.g. Mig1p), resulting in an *HXT2/4* expression window when glucose is present only in low concentrations (Özcan and Johnston 1996); interestingly, this window also seems to span xylose conditions (Figure 4C & D). Mig1p simultaneously affects *SUC2*: at low glucose concentrations SNF1 is activated and phosphorylates Mig1p (Figure 1B) leading to a derepression of the high-affinity hexose transporters *HXT2/4* and *SUC2* (Westholm, et al. 2008). Indeed, it was observed that xylose triggers the SNF1/Mig1p signaling pathway (Figure 4E) in the same manner that it triggers the low glucose concentration-sensing *HXT2/4p*. The behavior of the *SUC2p* biosensor (TMB3755) also matches that of a transcriptomics study on *S. cerevisiae* engineered for xylose utilization, which showed a peak expression of *SUC2* occurring during xylose conditions, leading the authors to hypothesize that xylose does not activate the glucose repression pathways in the same way as glucose does (Salusjärvi, et al. 2008).

TPS1/2 are known to be induced by stress conditions (including glucose limitation) (Winderickx, et al. 1996), but interestingly, the wild type biosensors (neither xylose transport nor assimilation) remained repressed with xylose 50 g/L after 6h (TMB3717-18; Brink, et al. (2016)). The current study, however, showed that in xylose condition the low FI subpopulations of these biosensors with just the transporter (TMB3727-28) were more repressed than the repression condition (glucose 40 g/L; Figure 3F-G). On the other hand, the corresponding biosensor strains with transporter and xylose pathway (TMB3757-58; Figure 4F-G) were induced in presence of xylose. This indicates that internalized and metabolized xylose has an effect on *TPS1/2* similar to that of low/limited glucose, while the lack of induction of these biosensors in the Gal2p mutant strains (TMB3727-28) is comparable to the signal of when they were submitted to YNB with no carbon source (S1 Supporting Information Table S7).

From a signaling pathway point-of-view (Figure 1), we could observe the following effects of xylose on TMB375X: the Snf3p/Rgt2p pathway was partially induced on xylose, that is the Snf3p regulated genes (*HXT2p/4p*) was induced whereas the Rgt2p side (*HXT1p*) was repressed; the SNF1/Mig1p pathway was induced (*SUC2p*); finally, the cAMP/PKA was

repressed (inversely proportional to *TPS1/2p,* which were activated). Interestingly, by taking this holistic view on the biosensor results, we observed that the pathway induction pattern fits with the known induction pattern of Protein Kinase A (PKA), a protein that to some extent is known to regulate all three of these pathways. PKA is activated by cAMP which in turn is activated by sensing of extra- and/or intracellular glucose (Peeters and Thevelein 2014, Santangelo 2006). Active PKA leads to activation of *HXT1p* (Jouandot, et al. 2011, Kim and Johnston 2006), repression of *SUC2p* (Gancedo, et al. 2015) and repression of *TPS1/2p* (Boy-Marcotte, et al. 1998, Roosen, et al. 2005). The results of the current study suggest, that since *HXT1p* was repressed, and *SUC2p* and *TPS1/2p* were induced on xylose (Figure 4) it follows that xylose cannot fully activate PKA. In that case, the PKA behavior may be one of the key signaling differences between glucose and xylose; this is graphically summarized in Figure 6. PKA is also inactivated during stress conditions, which subsequently triggers activation of the environmental stress response through e.g. Msn2p/4p (Smith, et al. 1998, Thevelein and De Winde 1999), meaning that the xylose utilizing strains may have an active stress response running simultaneous to the carbon metabolism which in turn would lead to a state of sub-optimal growth.

Furthermore, it is known that Hexokinase 2 (Hxk2p) has an important regulatory function in sugar signaling and glucose carbon catabolite repression, and is e.g. required both to fully induce *HXT1* during high glucose conditions (through Rgt1p), and to de-repress *SUC2* during low glucose conditions (through Mig1p) (Moreno and Herrero 2002, Özcan and Johnston 1995), cf. Figure 1B. *In vitro* studies have shown that Hxk2p is inactivated by D-xylose through an autophosphorylation at the active site (Fernandez, et al. 1986, Heidrich, et al. 1997); moreover, *HXK2* is repressed by Rgt1p in the absence of glucose (Palomino, et al. 2005), meaning that the low glucose-high xylose effect that we observed have two different mechanistic explanations with similar outcome when we consider Hxk2p as a key signaling regulator. The lack of signal in the *HXT1p* biosensors (TMB3722 & 3752) during conditions with xylose as sole carbon source (Figure 3 & 4) would then be explained by the fact that this transporter is repressed by low glucose levels (Figure 1B, Table 3) and that one of its inducers, Hxk2p, is inactivated by (intracellular) xylose. Furthermore, deletion studies have shown that genes of low-affinity hexose transporters (e.g. *HXT1*) were downregulated in Δ*hxk2* strains, whereas high-affinity transporters (e.g. *HXT2/4*) were upregulated (Petit, et al. 2000, Özcan and Johnston 1995). The observed signal for the *HXT2/4*p high-affinity

transporters on xylose in all the three strain series (TMB3713-14 Brink, et al. (2016); TMB3723-24, Figure 3; TMB3753-54, Figure 4), could, at least partly, also be explained in relation to Hxk2p: intracellular xylose inactivates hexokinase, which then de-represses the high-affinity transporters. However, the case seems to be slightly different for *SUC2p* - a gene that is also regulated by Hxk2p (Moreno and Herrero 2002) - which was not fully induced on xylose until strain TMB3755 (transporter + assimilation; Figure 4E vs. 3E). Studies have shown that Hxk2p only controls the long-term repression of *SUC2* on glucose (de Winde, et al. 1996, Sanz, et al. 1996), which, together with the fact that the *HXT* and *SUC2* genes are controlled by different signaling pathways (Snf3p/Rgt2p and *SNF1*/Mig1p respectively), could explain the different results of these biosensors.

It should also be noted that the observed overall decrease in population heterogeneity in TMB375X (transporter + assimilation) compared to TMB372X (transporter) might also suggest that the sugar signaling pathways are affected by intermediate metabolites formed from xylose during its catabolism, since the main difference between these strain series is the addition of the XR/XDH/XKS and *TAL1*/*TKL1* cassettes (Table 1). The recombinant xylose pathways shunt carbon to the glycolysis via the PPP, which means that the observed biosensor induction on xylose in the TMB375X strains (transporter + assimilation; Figure 4) can have resulted from signaling feedback from the lower glycolysis and central carbon metabolism.

Conclusions

We have identified two major problems in how xylose is sensed by *S. cerevisiae*: 1) xylose is not sensed extracellularly (TMB371X; Brink, et al. (2016)) and 2) xylose-utilizing strains produce a similar signal for high xylose as for low glucose. The consequences of xylose not being sensed in the extracellular space leads to a cascade of signaling reactions that involves all three sugar signaling pathways: for instance, if xylose is not sensed outside the cell it does not induce the extracellular receptors of the Snf3p/Rgt2 and cAMP/PKA pathways, which in turn does not trigger a complete expression of hexose transporters (mainly the low-affinity hexose transporters such as *HXT1* remain unexpressed) and inactivates PKA. Furthermore, a high xylose signal (which we postulate to be similar to a low-glucose signal) leads to an activation of the SNF1/Mig1p pathway by inactivating Hxk2p, allowing for the expression of

alternative-carbon utilization genes (e.g. *SUC2)*, while low-affinity hexose transporters again are repressed. This study also shows that the sensing of intracellular xylose changes when strains are engineered to transport, and to assimilate xylose, and implies that further studies aimed to improve xylose utilization in this yeast need to be performed in strains engineered to grow on xylose instead of wild type strains.

Abbreviations

FI: fluorescence intensity; GFP: Green Fluorescent Protein; OD: Optical Density; OE-PCR: overlap extension PCR; PCR: Polymerase Chain Reaction; PPP: pentose phosphate pathway; XDH: xylitol dehydrogenase; XK: xylulose kinase; XR: xylose reductase; YPD: Yeast Peptone Dextrose.

Competing interests

The authors declare that they have no competing interests.

Authors' contributions

KOO, MC and MGG designed the study. KOO performed the strain construction, enzymatic assays, flow cytometry analysis, data analysis, and drafted the initial manuscript. DB participated in the molecular biology work, strain construction, data analysis (e.g. the Gaussian Mixture modelling) and manuscript revision. CB participated in the data analysis and manuscript revision. LW designed and constructed the XK/XDH and TAL/TKL cassettes (pLWA plasmids). KOO and DB finalized the manuscript. MGG conceived the study and revised the manuscript. All authors read and approved the final manuscript.

Funding

This work was supported by The Swedish Research Council (Vetenskapsrådet) [grant number 2016-05297_VR], and The Brazilian National Council for Scientific and Technological Development (Conselho Nacional de Desenvolvimento Científico e Tecnológico) [scholarship awarded for KOO].

Acknowledgements

The authors would like to acknowledge Felipe G. Tueros for his assistance in generating some of the strains used in the study. The pRS62N_GAL2_N376F plasmid was kindly provided by Eckhard Boles (Goethe University, Frankfurt, Germany). We would also like to thank Irina Borodina, Vratislav Stovicek and Jochen Förster (Technical University of Denmark, Copenhagen, Denmark) for providing plasmids for the CRISPR-Cas9 system used in this study.

References

Alff-Tuomala S, Salusjärvi L, Barth D, Oja M, Penttilä M, Pitkänen J-P, Ruohonen L, Jouhten P. Xylose-induced dynamic effects on metabolism and gene expression in engineered *Saccharomyces cerevisiae* in anaerobic glucose-xylose cultures. *Appl Microbiol Biot* 2016;**100**: 969-85.

Apel AR, Ouellet M, Szmidt-Middleton H, Keasling JD, Mukhopadhyay A. Evolved hexose transporter enhances xylose uptake and glucose/xylose co-utilization in *Saccharomyces cerevisiae*. *Scientific reports* 2016;**6**.

Attfield PV, Bell PJ. Use of population genetics to derive nonrecombinant *Saccharomyces cerevisiae* strains that grow using xylose as a sole carbon source. *FEMS Yeast Res* 2006;**6**: 862-8.

Bergdahl B, Heer D, Sauer U, Hahn-Hägerdal B, van Niel EWJ. Dynamic metabolomics differentiates between carbon and energy starvation in recombinant *Saccharomyces cerevisiae* fermenting xylose. *Biotechnol Biofuels* 2012;**5**.

Boles E, Hollenberg CP. The molecular genetics of hexose transport in yeasts. *FEMS Microbiol Rev* 1997;**21**: 85-111.

Boy-Marcotte E, Perrot M, Bussereau F, Boucherie H, Jacquet M. Msn2p and Msn4p control a large number of genes induced at the diauxic transition which are repressed by cyclic AMP in *Saccharomyces cerevisiae*. *Journal of bacteriology* 1998;**180**: 1044-52.

Brat D, Boles E, Wiedemann B. Functional Expression of a Bacterial Xylose Isomerase in *Saccharomyces cerevisiae*. *Appl Environ Microb* 2009;**75**: 2304-11.

Brink DP, Borgström C, Tueros FG, Gorwa-Grauslund MF. Real-time monitoring of the sugar sensing in *Saccharomyces cerevisiae* indicates endogenous mechanisms for xylose signaling. *Microb Cell Fact* 2016;**15**: 183.

Bruinenberg PM, de Bot PH, van Dijken JP, Scheffers WA. The role of redox balances in the anaerobic fermentation of xylose by yeasts. *European journal of applied microbiology and biotechnology* 1983;**18**: 287-92.

Burnett RW. Accurate measurement of molar absorptivities. *J Res Nat Bur Stand A* 1972;**76**: 483.

Cadete RM, de las Heras AM, Sandström AG, Ferreira C, Gírio F, Gorwa-Grauslund MF, Rosa CA, Fonseca C. Exploring xylose metabolism in *Spathaspora* species: XYL1. 2 from *Spathaspora passalidarum* as the key for efficient anaerobic xylose fermentation in metabolic engineered *Saccharomyces cerevisiae*. *Biotechnol Biofuels* 2016;**9**: 167.

de Winde JH, Crauwels M, Hohmann S, Thevelein JM, Winderickx J. Differential Requirement of the Yeast Sugar Kinases for Sugar Sensing in Establishing the Catabolite-Repressed State. *The FEBS Journal* 1996;**241**: 633-43.

Farwick A, Bruder S, Schadeweg V, Oreb M, Boles E. Engineering of yeast hexose transporters to transport D-xylose without inhibition by D-glucose. *P Natl Acad Sci USA* 2014;**111**: 5159-64.

Feng X, Zhao H. Investigating glucose and xylose metabolism in *Saccharomyces cerevisiae* and *Scheffersomyces stipitis* via C-13 metabolic flux analysis. *AiChE Journal* 2013;**59**: 3195-202.

Fernandez R, Herrero P, Fernandez M, Moreno F. Mechanism of inactivation of hexokinase PII of *Saccharomyces cerevisiae* by D-xylose. *Microbiology* 1986;**132**: 3467-72.

Gancedo JM, Flores C-L, Gancedo C. The repressor Rgt1 and the cAMP-dependent protein kinases control the expression of the SUC2 gene in *Saccharomyces cerevisiae*. *Biochimica et Biophysica Acta (BBA)-General Subjects* 2015;**1850**: 1362-7.

Gietz RD, Schiestl RH. High-efficiency yeast transformation using the LiAc/SS carrier DNA/PEG method. *Nat Protoc* 2007;**2**: 31-4.

Gietz RD, Sugino A. New Yeast-*Escherichia coli* Shuttle Vectors Constructed with *In vitro* Mutagenized Yeast Genes Lacking six-Base Pair Restriction Sites. *Gene* 1988;**74**: 527-34.

Hahn-Hägerdal B, Karhumaa K, Fonseca C, Spencer-Martins I, Gorwa-Grauslund MF. Towards industrial pentose-fermenting yeast strains. *Appl Microbiol Biot* 2007a;**74**: 937-53.

Hahn-Hägerdal B, Karhumaa K, Jeppsson M, Gorwa-Grauslund MF. Metabolic engineering for pentose utilization in *Saccharomyces cerevisiaeBiofuels*: Springer, 2007b, 147-77.

Hamacher T, Becker J, Gardonyi M, Hahn-Hägerdal B, Boles E. Characterization of the xylose-transporting properties of yeast hexose transporters and their influence on xylose utilization. *Microbiol-Sgm* 2002;**148**: 2783-8.

Heidrich K, Otto A, Behlke J, Rush J, Wenzel K-W, Kriegel T. Autophosphorylation−Inactivation Site of Hexokinase 2 in *Saccharomyces cerevisiae*. *Biochemistry* 1997;**36**: 1960-4.

Hill J, Donald KAIG, Griffiths DE. DMSO-Enhanced Whole Cell Yeast Transformation. *Nucleic Acids Res* 1991;**19**: 5791-.

Ho NW, Chen Z, Brainard AP. Genetically engineered *Saccharomyces* yeast capable of effective cofermentation of glucose and xylose. *Appl Environ Microb* 1998;**64**: 1852-9.

Horecker BL, Kornberg A. The extinction coefficients of the reduced band of pyridine nucleotides. *J Biol Chem* 1948;**175**: 385-90.

Inoue H, Nojima H, Okayama H. High-Efficiency Transformation of *Escherichia coli* with Plasmids. *Gene* 1990;**96**: 23-8.

Jeffries T, Jin Y-S. Metabolic engineering for improved fermentation of pentoses by yeasts. *Appl Microbiol Biot* 2004;**63**: 495-509.

Jessop-Fabre MM, Jakočiūnas T, Stovicek V, Dai Z, Jensen MK, Keasling JD, Borodina I. EasyClone-MarkerFree: A vector toolkit for marker-less integration of genes into *Saccharomyces cerevisiae* via CRISPR-Cas9. *Biotechnol J* 2016;**11**: 1110-7.

Jin YS, Laplaza JM, Jeffries TW. *Saccharomyces cerevisiae* engineered for xylose metabolism exhibits a respiratory response. *Appl Environ Microb* 2004;**70**: 6816-25.

Jouandot D, Roy A, Kim JH. Functional dissection of the glucose signaling pathways that regulate the yeast glucose transporter gene (HXT) repressor Rgt1. *Journal of cellular biochemistry* 2011;**112**: 3268-75.

Kaniak A, Xue Z, Macool D, Kim J-H, Johnston M. Regulatory network connecting two glucose signal transduction pathways in *Saccharomyces cerevisiae*. *Eukaryot Cell* 2004;**3**: 221-31.

Kim J-H, Johnston M. Two glucose-sensing pathways converge on Rgt1 to regulate expression of glucose transporter genes in *Saccharomyces cerevisiae*. *J Biol Chem* 2006;**281**: 26144-9.

Kim J-H, Polish J, Johnston M. Specificity and regulation of DNA binding by the yeast glucose transporter gene repressor Rgt1. *Mol Cell Biol* 2003;**23**: 5208-16.

Kim SR, Ha S-J, Wei N, Oh EJ, Jin Y-S. Simultaneous co-fermentation of mixed sugars: a promising strategy for producing cellulosic ethanol. *Trends in biotechnology* 2012;**30**: 274-82.

Klimacek M, Krahulec S, Sauer U, Nidetzky B. Limitations in Xylose-Fermenting *Saccharomyces cerevisiae*, Made Evident through Comprehensive Metabolite Profiling and Thermodynamic Analysis. *Appl Environ Microb* 2010;**76**: 7566-74.

Kotyk A. Properties of the sugar carrier in baker's yeast. *Folia microbiologica* 1967;**12**: 121-31.

Kraakman LS, Winderickx J, Thevelein JM, de Winde JH. Structure-function analysis of yeast hexokinase: structural requirements for triggering cAMP signalling and catabolite repression. *Biochem J* 1999;**343**: 159-68.

Kwak S, Jin Y-S. Production of fuels and chemicals from xylose by engineered *Saccharomyces cerevisiae*: a review and perspective. *Microb Cell Fact* 2017;**16**: 82.

Kötter P, Amore R, Hollenberg CP, Ciriacy M. Isolation and characterization of the *Pichia stipitis* xylitol dehydrogenase gene, XYL2, and construction of a xylose-utilizing *Saccharomyces cerevisiae* transformant. *Curr Genet* 1990;**18**: 493-500.

Kötter P, Ciriacy M. Xylose Fermentation by *Saccharomyces cerevisiae*. *Appl Microbiol Biot* 1993;**38**: 776-83.

Limayem A, Ricke SC. Lignocellulosic biomass for bioethanol production: current perspectives, potential issues and future prospects. *Progress in Energy and Combustion Science* 2012;**38**: 449-67.

Lõoke M, Kristjuhan K, Kristjuhan A. Extraction of genomic DNA from yeasts for PCR-based applications. *Biotechniques* 2011;**50**: 325-+.

Matsushika A, Inoue H, Kodaki T, Sawayama S. Ethanol production from xylose in engineered *Saccharomyces cerevisiae* strains: current state and perspectives. *Appl Microbiol Biot* 2009;**84**: 37-53.

Moreno F, Herrero P. The hexokinase 2-dependent glucose signal transduction pathway of *Saccharomyces cerevisiae*. *FEMS Microbiol Rev* 2002;**26**: 83-90.

Mosley AL, Lakshmanan J, Aryal BK, Özcan S. Glucose-mediated phosphorylation converts the transcription factor Rgt1 from a repressor to an activator. *J Biol Chem* 2003;**278**: 10322-7.

Moysés DN, Reis VCB, Almeida JRMd, Moraes LMPd, Torres FAG. Xylose Fermentation by *Saccharomyces cerevisiae*: challenges and prospects. *International journal of molecular sciences* 2016;**17**: 207.

Mumberg D, Muller R, Funk M. Yeast Vectors for the Controlled Expression of Heterologous Proteins in Different Genetic Backgrounds. *Gene* 1995;**156**: 119-22.

Nijland JG, Shin HY, de Jong RM, De Waal PP, Klaassen P, Driessen AJ. Engineering of an endogenous hexose transporter into a specific D-xylose transporter facilitates glucose-xylose co-consumption in *Saccharomyces cerevisiae*. *Biotechnol Biofuels* 2014;**7**: 168.

Nijland JG, Vos E, Shin HY, Waal PP, Klaassen P, Driessen AJ. Improving pentose fermentation by preventing ubiquitination of hexose transporters in *Saccharomyces cerevisiae*. *Biotechnol Biofuels* 2016;**9**: 158.

Palomino A, Herrero P, Moreno F. Rgt1, a glucose sensing transcription factor, is required for transcriptional repression of the HXK2 gene in *Saccharomyces cerevisiae*. *Biochem J* 2005;**388**: 697-703.

Peeters K, Thevelein JM. Glucose sensing and signal transduction in *Saccharomyces cerevisiae. Molecular Mechanisms in Yeast Carbon Metabolism*: Springer, 2014, 21-56.

Petit T, Diderich JA, Kruckeberg AL, Gancedo C, Dam K. Hexokinase Regulates Kinetics of Glucose Transport and Expression of Genes Encoding Hexose Transporters in *Saccharomyces cerevisiae*. *Journal of Bacteriology* 2000; **182**: 6815–6818.

Raman M, Martin K. One solution for cloning and mutagenesis: In-Fusion® HD Cloning Plus. *Nature Methods* 2014;**11**.

Rizzi M, Harwart K, Erlemann P, Bui-Thanh N-A, Dellweg H. Purification and properties of the NAD+-xylitol-dehydrogenase from the yeast *Pichia stipitis*. *Journal of Fermentation and Bioengineering* 1989;**67**: 20-4.

Rolland F, Winderickx J, Thevelein JM. Glucose-sensing and-signalling mechanisms in yeast. *FEMS Yeast Res* 2002;**2**: 183-201.

Roosen J, Engelen K, Marchal K, Mathys J, Griffioen G, Cameroni E, Thevelein JM, De Virgilio C, De Moor B, Winderickx J. PKA and Sch9 control a molecular switch important for the proper adaptation to nutrient availability. *Mol Microbiol* 2005;**55**: 862-80.

Rudolf A, Baudel H, Zacchi G, Hahn-Hägerdal B, Lidén G. Simultaneous saccharification and fermentation of steam-pretreated bagasse using *Saccharomyces cerevisiae* TMB3400 and *Pichia stipitis* CBS6054. *Biotechnol Bioeng* 2008;**99**: 783-90.

Runquist D, Hahn-Hägerdal B, Bettiga M. Increased expression of the oxidative pentose phosphate pathway and gluconeogenesis in anaerobically growing xylose-utilizing *Saccharomyces cerevisiae*. *Microb Cell Fact* 2009;**8**: 1.

Salusjarvi L, Pitkanen JP, Aristidou A, Ruohonen L, Penttila M. Transcription analysis of recombinant *Saccharomyces cerevisiae* reveals novel responses to xylose. *Appl Biochem Biotech* 2006;**128**: 237-61.

Salusjärvi L, Kankainen M, Soliymani R, Pitkänen JP, Penttilä M, Ruohonen L. Regulation of xylose metabolism in recombinant *Saccharomyces cerevisiae*. *Microb Cell Fact* 2008;**7**.

Sambrook J, Russell DW. *Molecular cloning: a laboratory manual*: 3rd Edition. Cold Spring Harbor, New York: Cold Spring Harbor Laboratory Press, 2001.

Santangelo GM. Glucose signaling in *Saccharomyces cerevisiae*. *Microbiol Mol Biol R* 2006;**70**: 253-82.

Sanz P, Nieto A, Prieto JA. Glucose repression may involve processes with different sugar kinase requirements. *Journal of bacteriology* 1996;**178**: 4721-3.

Skoog K, Hahn-Hägerdal B. Xylose fermentation. *Enzyme Microb Tech* 1988;**10**: 66-80.

Smiley KL, Bolen PL. Demonstration of D-xylose reductase and D-xylitol dehydrogenase in *Pachysolen tannophilus*. *Biotechnology Letters* 1982;**4**: 607-10.

Smith A, Ward MP, Garrett S. Yeast PKA represses Msn2p/Msn4p-dependent gene expression to regulate growth, stress response and glycogen accumulation. *The EMBO journal* 1998;**17**: 3556-64.

Solis-Escalante D, Kuijpers NG, Nadine B, Bolat I, Bosman L, Pronk JT, Daran J-M, Pascale D-L. amdSYM, a new dominant recyclable marker cassette for *Saccharomyces cerevisiae*. *FEMS Yeast Res* 2013;**13**: 126-39.

Stovicek V, Borodina I, Forster J. CRISPR–Cas system enables fast and simple genome editing of industrial *Saccharomyces cerevisiae* strains. *Metabolic Engineering Communications* 2015;**2**: 13-22.

Thevelein JM, De Winde JH. Novel sensing mechanisms and targets for the cAMP–protein kinase A pathway in the yeast *Saccharomyces cerevisiae*. *Mol Microbiol* 1999;**33**: 904-18.

Thomas BJ, Rothstein R. Elevated Recombination Rates in Transcriptionally Active DNA. *Cell* 1989;**56**: 619-30.

Toivari MH, Salusjarvi L, Ruohonen L, Penttila M. Endogenous xylose pathway in *Saccharomyces cerevisiae*. *Appl Environ Microb* 2004;**70**: 3681-6.

Tomás-Cobos L, Casadomé L, Mas G, Sanz P, Posas F. Expression of the HXT1 low affinity glucose transporter requires the coordinated activities of the HOG and glucose signalling pathways. *J Biol Chem* 2004;**279**: 22010-9.

Uihlein A, Schebek L. Environmental impacts of a lignocellulose feedstock biorefinery system: an assessment. *Biomass and Bioenergy* 2009;**33**: 793-802.

van Maris A, Winkler A, Kuyper M, de Laat W, van Dijken J, Pronk J. Development of efficient xylose fermentation in *Saccharomyces cerevisiae*: xylose isomerase as a key component. *Biofuels* 2007: 179-204.

Westholm JO, Nordberg N, Murén E, Ameur A, Komorowski J, Ronne H. Combinatorial control of gene expression by the three yeast repressors Mig1, Mig2 and Mig3. *BMC genomics* 2008;**9**: 601.

Winderickx J, de Winde JH, Crauwels M, Hino A, Hohmann S, Van Dijck P, Thevelein JM. Regulation of genes encoding subunits of the trehalose synthase complex in *Saccharomyces cerevisiae*: Novel variations of STRE-mediated transcription control? *Mol Gen Genet* 1996;**252**: 470-82.

Zaldivar J, Borges A, Johansson B, Smits H, Villas-Bôas S, Nielsen J, Olsson L. Fermentation performance and intracellular metabolite patterns in laboratory and industrial xylose-fermenting *Saccharomyces cerevisiae*. *Appl Microbiol Biot* 2002;**59**: 436-42.

Zeng W-Y, Tang Y-Q, Gou M, Xia Z-Y, Kida K. Transcriptomes of a xylose-utilizing industrial flocculating *Saccharomyces cerevisiae* strain cultured in media containing different sugar sources. *AMB Express* 2016;**6**: 51.

Özcan S, Dover J, Johnston M. Glucose sensing and signaling by two glucose receptors in the yeast *Saccharomyces cerevisiae*. *The EMBO journal* 1998;**17**: 2566-73.
Özcan S, Johnston M. Three Different Regulatory Mechanisms Enable Yeast Hexose Transporter (Hxt) Genes to Be Induced by Different Levels of Glucose. *Mol Cell Biol* 1995;**15**: 1564-72.
Özcan S, Johnston M. Two different repressors collaborate to restrict expression of the yeast glucose transporter genes HXT2 and HXT4 to low levels of glucose. *Mol Cell Biol* 1996;**16**: 5536-45.
Özcan S, Vallier LG, Flick JS, Carlson M, Johnston M. Expression of the SUC2 gene of *Saccharomyces cerevisiae* is induced by low levels of glucose. *Yeast* 1997;**13**: 127-37.

Figure captions

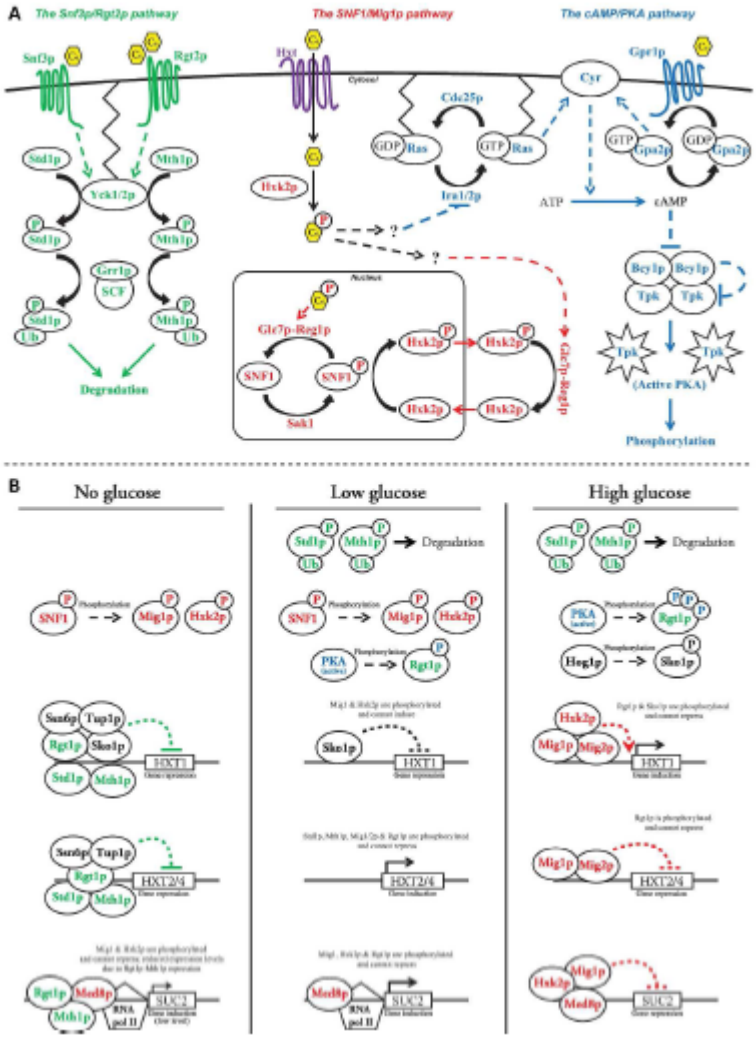

Figure 1. A: The three main glucose signalling pathways in *S. cerevisiae.* The Snf3p/Rgt2p pathway (green) controls expression of hexose transporters and responds to extracellular glucose (yellow hexagons with C_6); the SNF1/Mig1p pathway (red) controls expression of genes related to utilization of alternative carbon sources and senses intracellular phosphorylated (P) glucose; the cAMP/PKA pathway (blue) controls homeostasis and stress response and senses both extra- and intracellular glucose. Solid arrows represent reactions/transport and dashed arrows represent induction (arrowhead) or repression (hammerhead). This figure was adapted from a previous study (Brink, et al. 2016). B: Known induction/repression effects on the *HXT1*, *HXT2/4* and *SUC2* genes during absence of glucose, low glucose (typically <1 g/L) and high glucose conditions (typically >10 g/L). Note

that Mig1p/2p are known to act redundantly on their targets, meaning that both enzymes are normally not needed for target gene induction.

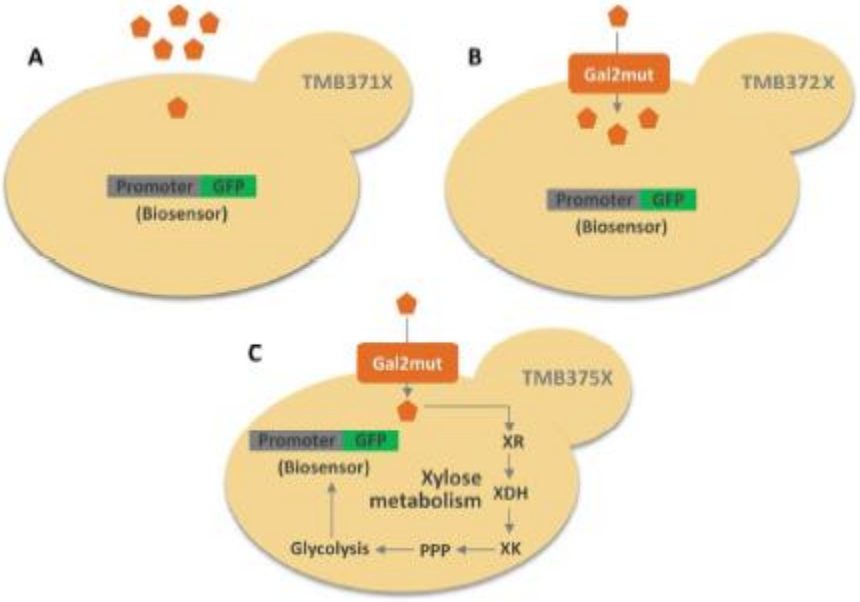

Figure 2. Schematic representation of the different biosensors strains. The biosensors were previously analyzed in TMB371X strains lacking xylose transport (i.e. no Gal2mut transporter) and assimilation (Brink, et al. 2016)(A). In this study, the biosensors were further evaluated with the overexpression of a xylose transporter (Gal2mut) in TMB372X strains (B). In the third case, a pathway for xylose utilization was added to the strains with Gal2mut transporter, resulting in the TMB375X strains (C).

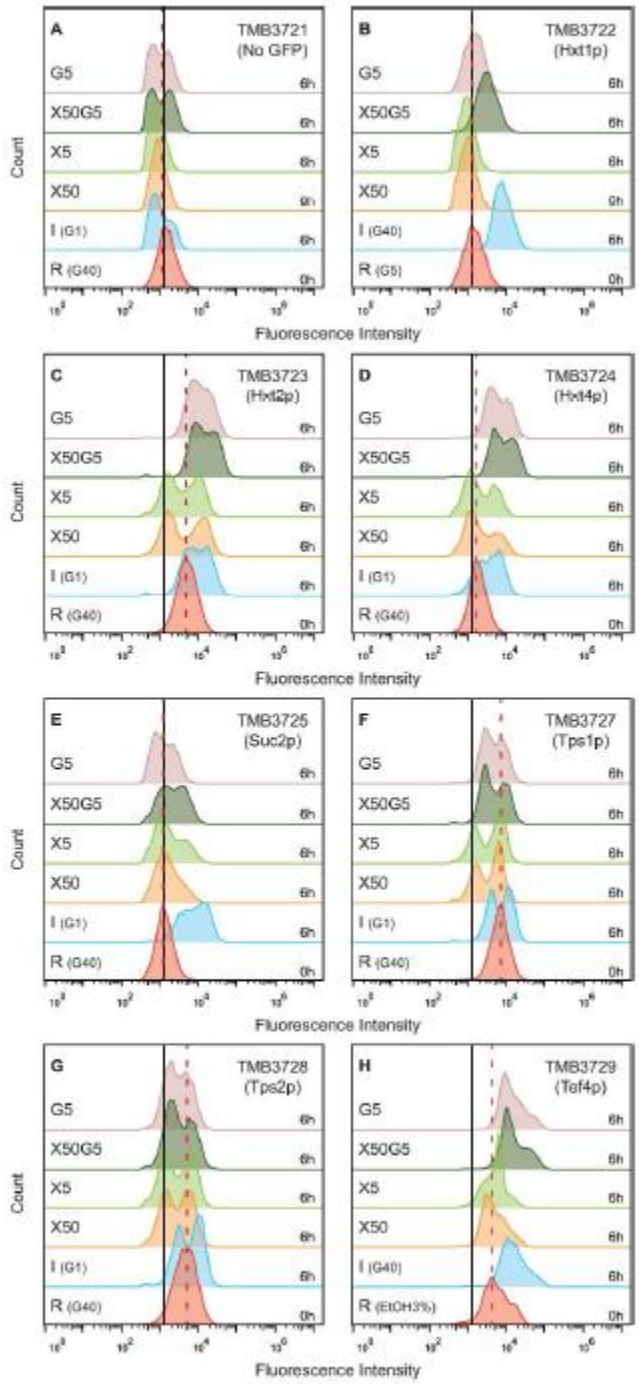

Figure 3. Histograms from flow cytometry analysis in microtiter platers of TMB372X strains in different conditions after 6 h. R: repression condition (see Table 3); I: induction condition (see Table 3); X50: xylose 50 g/L; X5: xylose 5 g/L; X50G5: xylose 50 g/L with glucose 5 g/L; G5: glucose 5 g/L. Black line is the reference for the auto-fluorescence intensity based on the negative control (TMB3721). The red dotted line marks the repression condition intensity

for each biosensor. The histograms are displayed in the figure are single replicates and are representative of their corresponding biological and technical replicates.

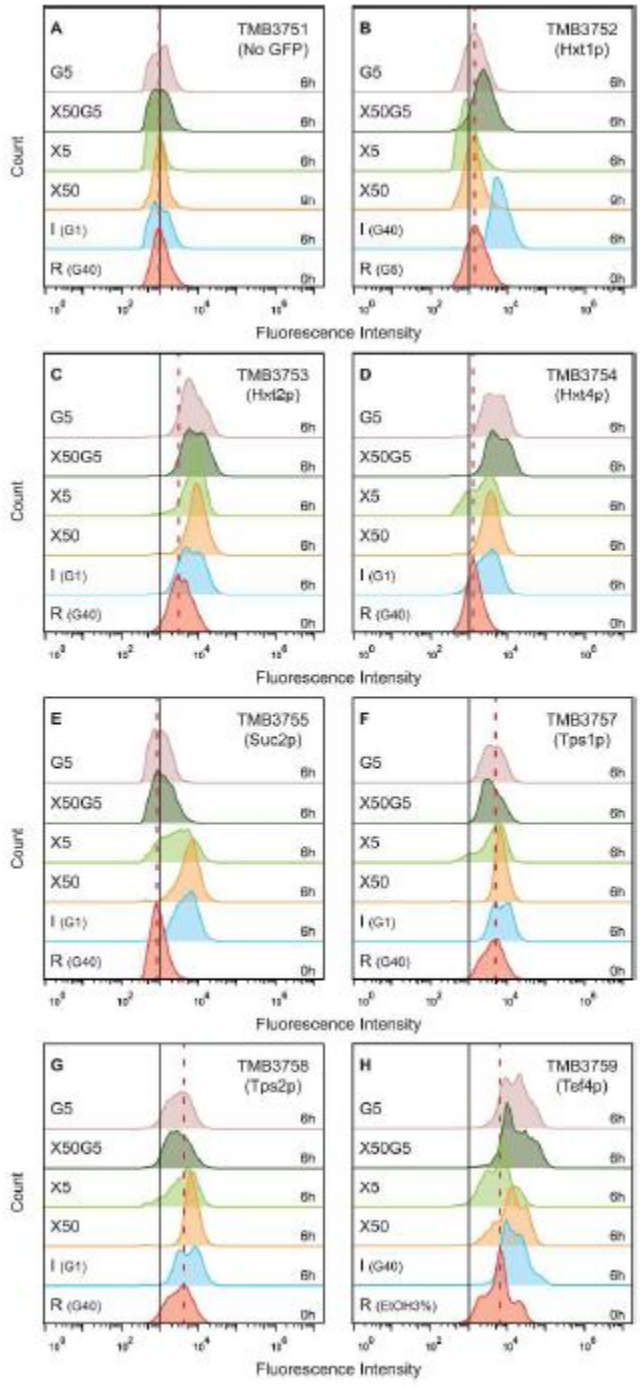

Figure 4. Histograms from flow cytometry analysis in microtiter platers of TMB375X strains in different conditions after 6 h: R: repression condition (see Table 3); I: induction condition

(see Table 3); X50: xylose 50 g/L; X5: xylose 5 g/L; X50G5: xylose 50 g/L with glucose 5 g/L; G5: glucose 5 g/L. Black line is the reference for auto-fluorescence intensity based on the negative control (TMB3751). The red dotted line marks the repression condition intensity foreach biosensor. The histograms are displayed in the figure are single replicates and are representative of their corresponding biological and technical replicates.

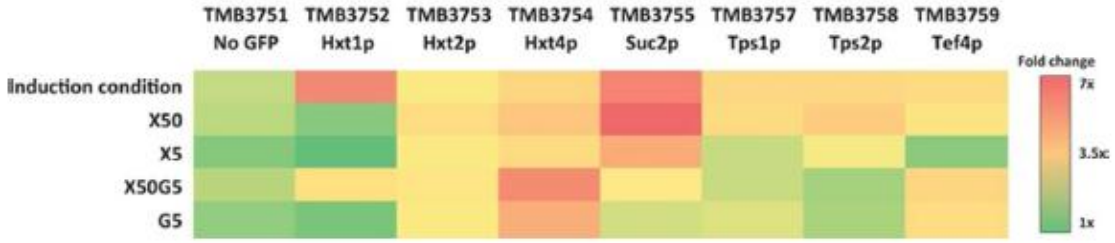

Figure 5. Heat map of the GFP fluorescence intensity (FI) of the TMB375X (transporter + assimilation) strains with the FI fold change from 0h to 6h. The different conditions were: induction condition (see Table 3), xylose 50 g/L (X50), xylose 5 g/L (X5), xylose 50 g/L with glucose 5 g/L (X50G5), and glucose 5 g/L (G5). The heat map values were taken from the average of the geometric mean-FI of all the biological triplicates (including the technical duplicates).

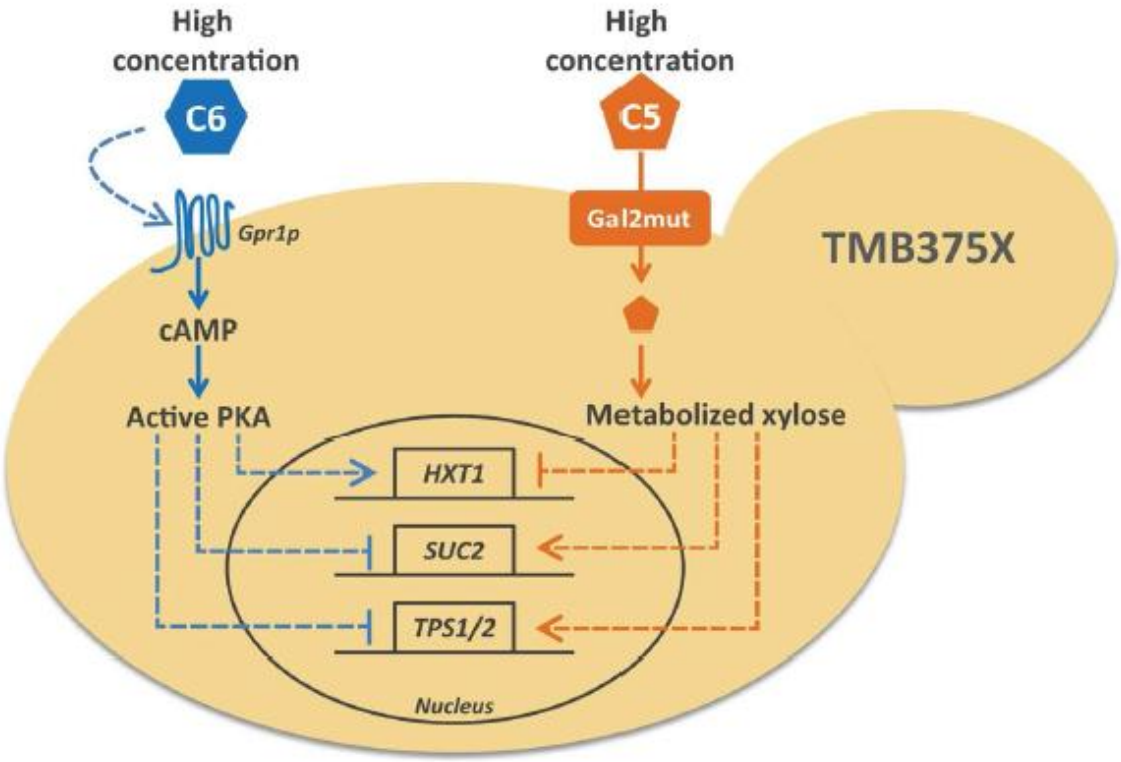

Figure 6. The effect of glucose-activated PKA on the signaling system compared to the observed effect of high xylose concentrations in the TMB375X (transporter + assimilation) strains. For *HXT1*, *SUC2* and *TPS1*/2 the signal response of high xylose is the direct opposite of that high glucose. From this it is hypothesized that high concentrations of xylose is sensed as low concentrations glucose by *S. cerevisiae* (see the *Discussion* section for details). Solid arrows: reactions/transport; dashed arrows: induction (arrowhead) or repression (hammerhead). Note that PKA is not necessarily the only regulator of these genes (cf. Figure 1).

Table 1. Yeast strains constructed and/or utilized in this study

Strain	Relevant genotype	Reference
W303-1A	*MATa trp1-1 leu2-3,112 his3-11 ade2-1 ura3-1 can1-100*	Thomas and Rothstein (1989); ATCC® 208352
TMB3700	W303-1A; TRP1 HIS3, *ura3::M3499 (ADE2)*	Brink, et al. (2016)
TMB370X series		
TMB3701	TMB3700; *can1::YIp211*	Brink et al., (unpublished)
TMB3702	TMB3700; *can1::YIpGFP−Hxt1p*	
TMB3703	TMB3700; *can1::YIpGFP−Hxt2p*	
TMB3704	TMB3700, *can1::YIpGFP−Hxt4p*	
TMB3705	TMB3700; *can1::YIpGFP−Suc2p*	
TMB3707	TMB3700; *can1::YIpGFP−Tps1p*	
TMB3708	TMB3700; *can1::YIpGFP−Tps2p*	
TMB3709	TMB3700; *can1::YIpGFP−Tef4p*	
TMB371X series		
TMB3711	TMB3701; *can1::YIp211; SPB1/PBN1::YIp128*	Brink, et al. (2016)
TMB3712	TMB3702; *can1::YIpGFP−Hxt1p; SPB1/PBN1::YIp128*	
TMB3713	TMB3703; *can1::YIpGFP−Hxt2p; SPB1/PBN1::YIp128*	
TMB3714	TMB3704; *can1::YIpGFP−Hxt4p; SPB1/PBN1::YIp128*	
TMB3715	TMB3705; *can1::YIpGFP−Suc2p; SPB1/PBN1::YIp128*	
TMB3717	TMB3707; *can1::YIpGFP−Tps1p; SPB1/PBN1::YIp128*	
TMB3718	TMB3708; *can1::YIpGFP−Tps2p; SPB1/PBN1::YIp128*	
TMB3719	TMB3709; *can1::YIpGFP−Tef4p; SPB1/PBN1::YIp128*	
TMB372X series		
TMB3721	TMB3701; *SPB1/PBN1::YIp128GAL2mut*	This study
TMB3722	TMB3702; *SPB1/PBN1::YIp128GAL2mut*	
TMB3723	TMB3703; *SPB1/PBN1::YIp128GAL2mut*	
TMB3724	TMB3704; *SPB1/PBN1::YIp128GAL2mut*	
TMB3725	TMB3705; *SPB1/PBN1::YIp128GAL2mut*	
TMB3727	TMB3707; *SPB1/PBN1::YIp128GAL2mut*	
TMB3728	TMB3708; *SPB1/PBN1::YIp128GAL2mut*	
TMB3729	TMB3709; *SPB1/PBN1::YIp128GAL2mut*	
TMB375X series		
TMB3751	TMB3721; *Vac17/MRC1::TKL-TAL*[1]*; Chr X-2/XI-5/XII-4::XR-XDH-XK*[2]	This study
TMB3752	TMB3722; *Vac17/MRC1::TKL-TAL; Chr X-2/XI-5/XII-4::XR-XDH-XK*	
TMB3753	TMB3723; *Vac17/MRC1::TKL-TAL; Chr X-2/XI-5/XII-4::XR-XDH-XK*	
TMB3754	TMB3724; *Vac17/MRC1::TKL-TAL; Chr X-2/XI-5/XII-4::XR-XDH-XK*	
TMB3755	TMB3725; *Vac17/MRC1::TKL-TAL; Chr X-2/XI-5/XII-4::XR-XDH-XK*	
TMB3757	TMB3727; *Vac17/MRC1::TKL-TAL; Chr X-2/XI-5/XII-4::XR-XDH-XK*	
TMB3758	TMB3728; *Vac17/MRC1::TKL-TAL; Chr X-2/XI-5/XII-4::XR-XDH-XK*	
TMB3759	TMB3729; *Vac17/MRC1::TKL-TAL; Chr X-2/XI-5/XII-4::XR-XDH-XK*	

[1] *TKL-TAL* = p*FBA1-TKL1*-t*PDC1*, p*TPI1-TAL1*-t*CPS1*

[2] *XR-XDH-XK* = p*TDH3-SpXYL1.2*-t*ADH1*, p*TEF1-SsXDH*-t*GPM1*, p*PGI1-XKS1*-t*PYK1*

Table 2. Plasmids used in this study

Plasmid	Relevant genotype	Reference
YIplac128	*AmpR; LEU2*	Gietz and Sugino (1988)
p426-GPD	*URA3; TDH3*p-*CYC1*t	Mumberg, et al. (1995)
YIpRC5	*URA3; TDH3p-XYL1-ADH1t, PGK1p-XYL2-PGK1t; SpXYL1.2* (from *S. passalidarum* UFMG-CM-Y469)	Cadete, et al. (2016)
pUG-amdSYM	*AmpR; AnTEF2p-amdSYM-AnTEF2t* (from *Aspergillus nidulans*)	Solis-Escalante, et al. (2013)
pRS62N_GAL2_N376F	*HXT7*p- *GAL2_N376F-CYC1*t	Farwick, et al. (2014)
YIplac128-GAL2_N376F	YIplac128*: TDH3*p- *GAL2_N376F-CYC1*t	This study
pCfB2312	*TEF*p-*Cas9-CYC1*t; *kanMX*	Stovicek, et al. (2015)
pCfB2899	X-2-MarkerFree backbone	Jessop-Fabre, et al. (2016)
pCfB3037	XI-5- MarkerFree backbone	Jessop-Fabre, et al. (2016)
pCfB3040	XII-4- MarkerFree backbone	Jessop-Fabre, et al. (2016)
pCfB3053	*CRISPR-cas9 gRNA* targeting the X-2 (NCA3/NSF1), XI-5 (FRE2/COS9) and XII-4 (NIT3/YLR352W) regions; *natMX*	Jessop-Fabre, et al. (2016)
pLWA19	p*FBA1-TKL1*-t*PDC1*, p*TPI1-TAL1*-t*CPS1; amdSYM*	This study
pLWA20	YIp-*TDH3p-XYL-ADH1t-TEF1p-XDH-GPM1t-PGI1p-XKS1-PYK1t*;URA3	This study
pLWA26	*gRNA-VAC17/MRC1; natMX*	This study
pLWA31	pCfB3037; p*TDH3-SpXYL1.2*-t*ADH1*, p*TEF1-SsXDH*-t*GPM1*, p*PGI1-XKS1*-t*PYK1*	This study
pLWA32	pCfB2899; p*TDH3-SpXYL1.2*-t*ADH1*, p*TEF1-SsXDH*-t*GPM1*, p*PGI1-XKS1*-t*PYK1*	This study
pLWA33	pCfB3040; p*TDH3-SpXYL1.2*-t*ADH1*, p*TEF1-SsXDH*-t*GPM1*, p*PGI1-XKS1*-t*PYK1*	This study

Table 3. Biosensor induction and repression condition and cultivation time used in the study, based on and modified from our previously established protocol (Brink, et al. 2016).

Strain	Promoter	Function	Signaling pathway	Repression condition	Induction condition
TMB37X1	Empty plasmid	Negative control	-	-	-
TMB37X2	*HXT1*p	Low−affinity hexose transporter	Snf3p/Rgt2p	Glucose 5g/L (14 h)	Glucose 40g/L (6 h)
TMB37X3	*HXT2*p	High−affinity hexose transporter	Snf3p/Rgt2p	Glucose 40g/L (14 h)	Glucose 1g/L (6 h)
TMB37X4	*HXT4*p	High−affinity hexose transporter	Snf3p/Rgt2p	Glucose 40g/L (14 h)	Glucose 1g/L (6 h)
TMB37X5	*SUC2*p	Invertase	SNF1/Mig1p	Glucose 40g/L (14 h)	Glucose 1g/L (6 h)
TMB37X7	*TPS1*p	Trehalose‑6‑phosphate synthase	cAMP/PKA	Glucose 40g/L (14 h)	Glucose 1g/L (6 h)
TMB37X8	*TPS2*p	Trehalose-6-phosphate phosphatase	cAMP/PKA	Glucose 40g/L (14 h)	Glucose 1g/L (6 h)
TMB37X9	*TEF4*p	Translation elongation factor	cAMP/PKA	EtOH 3% (v/v) (26 h)	Glucose 40g/L (6 h)